Science of the Total Environment 825 (2022) 153907

Contents lists available at ScienceDirect

Science of the Total Environment

journal homepage: www.elsevier.com/locate/scitotenv

Impact of permeate flux and gas sparging rate on membrane performance and process economics of granular anaerobic membrane bioreactors

Sergi Vinardell [a,b,*], Lucie Sanchez [b], Sergi Astals [a], Joan Mata-Alvarez [a,c], Joan Dosta [a,c], Marc Heran [b], Geoffroy Lesage [b]

[a] Department of Chemical Engineering and Analytical Chemistry, University of Barcelona, 08028 Barcelona, Spain
[b] Institut Européen des Membranes (IEM), Université de Montpellier, CNRS, ENSCM, 34090 Montpellier, France
[c] Water Research Institute, University of Barcelona, 08028 Barcelona, Spain

HIGHLIGHTS

- The impact of flux and gas sparging rate on granular AnMBRs was analysed.
- Flux and SGD had a direct effect on membrane fouling.
- Flux and SGD did not impact dissolved and colloidal organic matter rejection.
- Membrane flux of 7.8 LMH and SGD of 0.5 $m^3\ m^{-2}\ h^{-1}$ was the most economical option.
- Electricity and membrane cost were the most sensitive economic parameters.

GRAPHICAL ABSTRACT

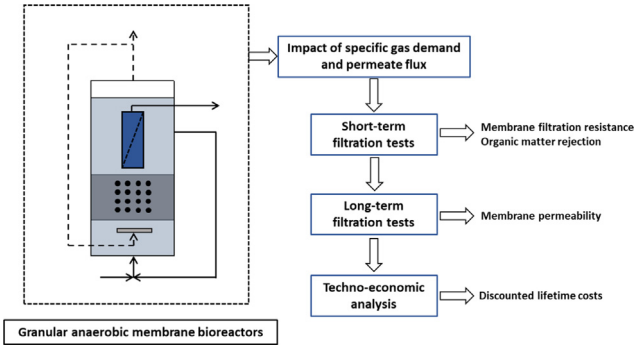

ARTICLE INFO

Article history:
Received 14 December 2021
Received in revised form 11 February 2022
Accepted 12 February 2022
Available online 17 February 2022

Editor: Huu Hao Ngo

Keywords:
Anaerobic membrane bioreactor (AnMBR)
Membrane fouling
Membrane rejection
Upflow anaerobic sludge blanket
Dissolved organic matter
Techno-economic analysis

ABSTRACT

This research investigated the impact of permeate flux and gas sparging rate on membrane permeability, dissolved and colloidal organic matter (DCOM) rejection and process economics of granular anaerobic membrane bioreactors (AnMBRs). The goal of the study was to understand how membrane fouling control strategies influence granular AnMBR economics. To this end, short- and long-term filtration tests were performed under different permeate flux and specific gas demand (SGD) conditions. The results showed that flux and SGD conditions had a direct impact on membrane fouling. At normalised fluxes (J_{20}) of 4.4 and 8.7 $L\ m^{-2}\ h^{-1}$ (LMH) the most favourable SGD condition was 0.5 $m^3\ m^{-2}\ h^{-1}$, whereas at J_{20} of 13.0 and 16.7 LMH the most favourable SGD condition was 1.0 $m^3\ m^{-2}\ h^{-1}$. The flux and the SGD did not have a direct impact on DCOM rejection, with values ranging between 31 and 44%. The three-dimensional excitation-emission matrix fluorescence (3DEEM) spectra showed that protein-like fluorophores were predominant in mixed liquor and permeate samples (67–79%) and were retained by the membrane (39–50%). This suggests that protein-like fluorophores could be an important foulant for these systems. The economic analysis showed that operating the membranes at moderate fluxes (J_{20} = 7.8 LMH) and SGD (0.5 $m^3\ m^{-2}\ h^{-1}$) could be the most favourable alternative. Finally, a sensitivity analysis illustrated that electricity and membrane cost were the most sensitive economic parameters, which highlights the importance of reducing SGD requirements and improving membrane permeability to reduce costs of granular AnMBRs.

* Corresponding author at: Department of Chemical Engineering and Analytical Chemistry, University of Barcelona, 08028 Barcelona, Spain.
E-mail address: svinardell@ub.edu (S. Vinardell).

http://dx.doi.org/10.1016/j.scitotenv.2022.153907

1. Introduction

Wastewater treatment plants (WWTP) are undergoing a transformative process where the energy consumption is reduced, the recovery of resources is maximised and the quality of the treated sewage is improved (McCarty et al., 2011). Membrane technologies play an important role in this transition since these technologies allow obtaining high-quality effluents free of suspended solids and pathogens with a high potential for their reuse (Krzeminski et al., 2017). Anaerobic membrane bioreactor (AnMBR) is an emerging technology for municipal sewage treatment that combines anaerobic digestion and membrane separation (Vinardell et al., 2020). This technology has a double positive connotation since it converts the sewage organic matter into methane-rich biogas and provides an excellent retention of the slow-growing anaerobic biomass into the bioreactor with a direct impact on process performance and effluent quality (Ozgun et al., 2013; Stazi and Tomei, 2018).

Several studies have shown the potential of AnMBRs to achieve high organic matter removals with competitive treatment costs (Pretel et al., 2014; Shoener et al., 2016; Vinardell et al., 2021). The technical and economic competitiveness of AnMBR has led to its full-scale implementation for the treatment of different types of industrial wastewater, including alcohol production stillage or food processing wastewater (Dereli et al., 2012; Zhen et al., 2019). However, AnMBR technology still needs to overcome some limitations before widespread implementation in WWTPs, such as membrane fouling, process temperature or low sewage organic matter concentration. Among these limitations, membrane fouling stands as one of the main challenges for full-scale application since it has a large influence on the technical and economic feasibility of the technology (Anjum et al., 2021; De Vela, 2021; Ji et al., 2021). Membrane fouling is a dynamic process that involves the interaction of organic and inorganic foulants with the membrane, which results in a progressive decrease of the membrane permeability (Meng et al., 2017). The decrease of membrane permeability leads to complex chemical and physical cleaning protocols that have a direct impact on the membrane lifetime and operating costs (Aslam et al., 2017; Dong et al., 2016). Furthermore, membrane permeability reduction also increases the AnMBR capital costs since larger membrane areas would be necessary as a result of the reduced flux. Therefore, the development of configurations and operational strategies able to reach an efficient control of membrane fouling is crucial to achieve relatively high fluxes without an excessive consumption of energy and chemicals.

Different configurations have been proposed in the literature to reduce membrane fouling in AnMBRs (Maaz et al., 2019; Song et al., 2018). The granular AnMBR, which is configured as an upflow anaerobic sludge blanket (UASB), is an interesting alternative to improve fouling control in AnMBRs and improve its full-scale applicability (Chen et al., 2017; Gouveia et al., 2015a; Martin-Garcia et al., 2011). In this configuration, the sewage is fed through the bottom of the bioreactor where a dense granular sludge with good settling characteristics is established. The membrane is typically submerged in an external tank or at the top of the bioreactor to reduce the concentration of solids nearby the membrane. The lower solids concentration close to the membrane aims to reduce cake layer formation and improve membrane fouling control in comparison with AnMBRs configured as continuous stirred tank reactors (Chen et al., 2016; Wang et al., 2018). However, the granular AnMBR system still presents some challenges concerning membrane fouling control. In granular AnMBR, the membrane is in contact with fine particles that are washed out from the granular sludge bed. The removal of these particles from the zones surrounding the membrane is challenging since they feature a poor settleability and back-transport characteristics (Gouveia et al., 2015b). The accumulation of these particles close to the membrane can reduce its permeability since microparticles have been reported to play an important role in AnMBR membrane fouling (Yao et al., 2020; Zhou et al., 2019). Accordingly, it is important to look for strategies able to scour and reduce the concentration of fine solids and colloidal organic matter close to the membrane.

Gas sparging is the most used strategy to control membrane fouling in AnMBRs (Fox and Stuckey, 2015; Robles et al., 2013). Gas sparging rates between 0.2 and 2 $m^3 m^{-2} h^{-1}$ have been reported in granular AnMBR systems treating municipal sewage (Gouveia et al., 2015a; Wang et al., 2018). The selection of the sparging rate should consider not only the energy consumption, but also the flux under which the membrane is operated since it also affects the extent of fouling. Wang et al. (2018) evaluated the impact of gas sparging rate on membrane fouling control and energy consumption of a granular AnMBR system. Continuous and intermittent gas sparging regimes as well as different membrane filtration modes were evaluated. Wang et al. (2018) demonstrated the importance of gas sparging regime, permeate flux and filtration mode on membrane permeability and energy consumption of the granular AnMBR system. However, this study did not evaluate how the different fouling control strategies could influence the costs of the system. In this regard, an economic analysis including all the costs influenced by the gas sparging rate and permeate flux (e.g. energy consumption, membrane purchase, consumption of chemicals, membrane replacement) is important to holistically evaluate the potential of AnMBR technology for municipal sewage treatment. To the best of the authors' knowledge, the coupling effect of gas sparging rate and permeate flux on capital and operating costs of granular AnMBRs has not yet been evaluated. Accordingly, further research is needed to understand under which sparging rate conditions the granular AnMBR permeate flux can be sustained at an optimum treatment cost.

This study aims to analyse the impact of permeate flux and gas sparging rate on membrane permeability, dissolved and colloidal organic matter (DCOM) rejection and economic feasibility of granular AnMBR systems. Short-term filtration tests were conducted to evaluate the variation of fouling resistance and DCOM rejection for different flux and gas sparging conditions. Subsequently, long-term filtration tests were carried out for the most favourable sparging rate conditions for each flux. The permeability results from the long-term filtration tests were used to conduct an economic analysis to determine the influence of the different membrane fouling control strategies on granular AnMBR economics. The ultimate goal is to understand how the interdependence of different permeate flux and gas sparging rate conditions influence membrane fouling and process economics of granular AnMBRs.

2. Materials and methods

2.1. Granular anaerobic sludge source

The granular anaerobic sludge used in the short- and long-term filtration tests was collected from a full-scale anaerobic reactor treating wastewater from a recycled paper processing factory (Laveyron, France). The anaerobic granular sludge had a total solids (TS) concentration of 90.6 ± 2.6 g L^{-1} with a volatile solids (VS) fraction of 77.0 ± 0.9%. The main characteristics of the sludge are shown in Table S1 of the supplementary material. The anaerobic granular sludge was kept refrigerated at 4 °C before its use.

2.2. Experimental set-up

The experimental set-up for the filtration tests consisted of a cuboid tank (282 × 100 × 900 mm) with a working volume of 17 L. The experimental set-up was designed to simulate hydrodynamic conditions of a granular AnMBR system. Three flat-sheet membrane modules with a total membrane area of 0.22 m^2 were submerged in the tank. Each membrane module consisted of two polyvinylidene difluoride (PVDF) microfiltration membranes (Amogreentech, South Korea) with a pore size of 0.3 μm. The permeate was withdrawn using a peristaltic pump (Longer Pump, China). A pressure sensor (Keller, Switzerland) was connected in the permeate line to record the transmembrane pressure (TMP). The permeate was returned back to the tank after the pressure was recorded. A peristaltic pump (Longer Pump, China) was used to recirculate the liquor from the top to the bottom of the tank to provide a liquid upflow velocity of 0.8 m h^{-1}, which is a typical liquid upflow velocity in granular AnMBR systems (Wang et al., 2020, 2018). This recirculation provided additional turbulence in the filtration

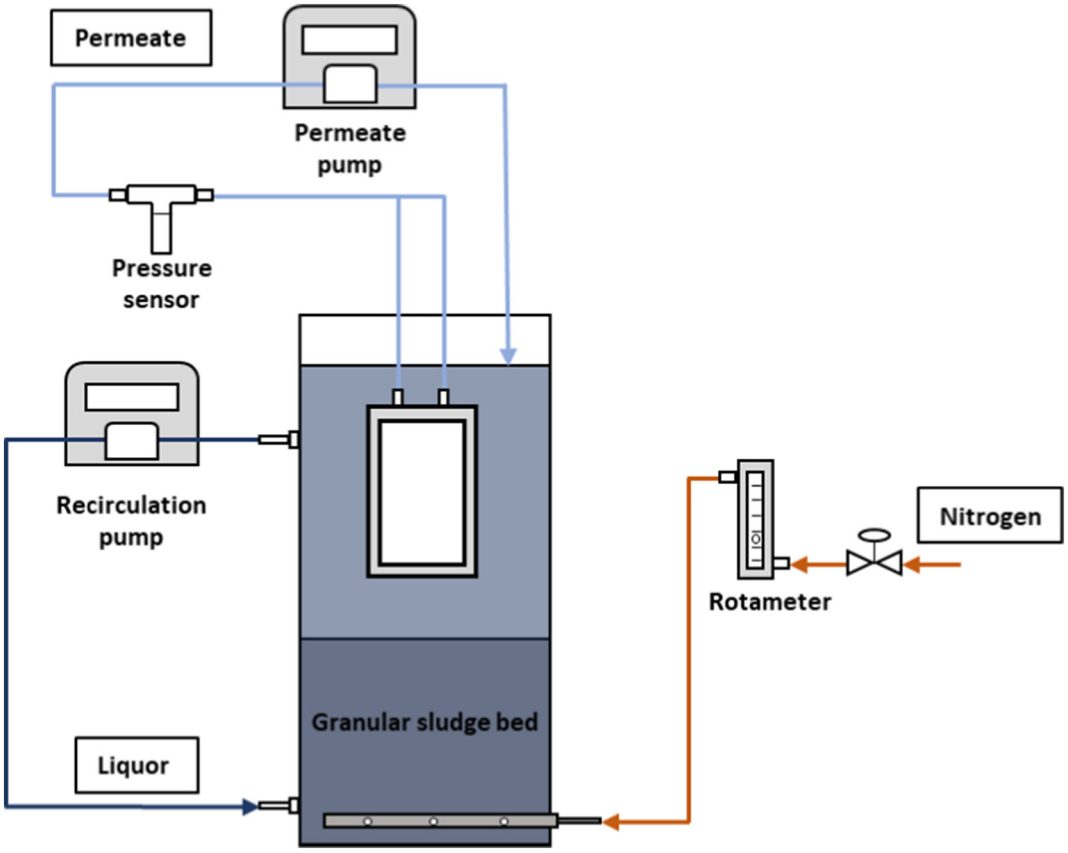

Fig. 1. Schematic representation of the experimental set-up used for the short- and long-term filtration tests.

zone, which is important to reduce the accumulation of fine solids and colloidal organic matter close to the membrane (Gouveia et al., 2015a). Pure nitrogen (99.9%) was used for gas sparging. The nitrogen was introduced at the bottom of the tank through three holes (d = 1.5 mm) that allowed a homogenous distribution of the gas throughout the tank's height. A rotameter flow meter (Krohne Group, Germany) was connected in the gas line to have a manual record of the nitrogen flow rate. The flow rate was adjusted by means of a regulating valve (Linde Engineering, Germany). A schematic representation of the experimental set-up can be found in Fig. 1.

Before each filtration test, the anaerobic granular sludge was diluted with distilled water to perform the filtration tests under controlled solids concentration conditions. The TS and VS concentrations in the tank ranged from 8.6 to 9.9 g TS L^{-1} and from 6.5 to 7.4 g VS L^{-1} for the filtration tests (Table S2 of the supplementary material).

2.3. Short-term filtration tests

Short-term filtration tests were conducted to evaluate the impact of flux and gas sparging rate on membrane permeability and DCOM rejection. Short-term filtration tests have been widely used in previous AnMBR studies as screening tool to determine the impact of membrane operational conditions on filtration performance under reproducible conditions (Fox and Stuckey, 2015; Odriozola et al., 2021; Ruigómez et al., 2016). Four specific gas demand (SGD) intensities (0.25, 0.5, 1.0 and 2.0 $m^3\ m^{-2}\ h^{-1}$) and four flux conditions (5, 10, 15 and 20 L $m^{-2}\ h^{-1}$ (LMH)) were evaluated in the short-term filtration tests. The SGD and flux conditions were selected based on available literature (Ruigómez et al., 2016; Wang et al., 2018). The SGD conditions are reported at normal conditions of pressure and temperature. Table 1 shows the fluxes and their normalised experimental values at 20 °C for each SGD condition.

The experimental cycle for the short-term filtration tests comprised four different stages: (1) distilled water filtration to determine the membrane filtration resistance, (2) granular sludge filtration to determine the total filtration resistance, (3) physical cleaning of the membrane with tap water and (4) chemical cleaning of the membrane with a 0.2% sodium hypochlorite solution for 2 h. These four stages were repeated for each flux. The total filtration resistance (Stage 2) for each SGD condition was obtained with a SGD step method adapted from Ruigómez et al. (2016). Specifically, Ruigómez et al. (2016) used the step method proposed by Le Clech et al. (2003) to evaluate the impact of different rotational velocities (fouling

Table 1
Permeate fluxes and their normalised values at 20 °C for each SGD and flux condition evaluated in the short-term filtration tests. Errors represent standard deviations (n = 18). No statistical difference was observed between the fluxes for the different SGDs at a specific flux condition (p > 0.05).

		SGD_1 (0.25 $m^3\ m^{-2}\ h^{-1}$)	SGD_2 (0.5 $m^3\ m^{-2}\ h^{-1}$)	SGD_3 (1.0 $m^3\ m^{-2}\ h^{-1}$)	SGD_4 (2.0 $m^3\ m^{-2}\ h^{-1}$)
$Flux_1$	$J_{T,1}$ (LMH)	4.8 ± 0.2	4.8 ± 0.3	4.7 ± 0.1	4.7 ± 0.1
	$J_{20,1}$ (LMH)	4.4 ± 0.3	4.4 ± 0.3	4.3 ± 0.2	4.4 ± 0.2
$Flux_2$	$J_{T,2}$ (LMH)	9.6 ± 0.2	9.6 ± 0.1	9.6 ± 0.2	9.5 ± 0.3
	$J_{20,2}$ (LMH)	8.7 ± 0.2	8.8 ± 0.2	8.7 ± 0.2	8.6 ± 0.3
$Flux_3$	$J_{T,3}$ (LMH)	14.1 ± 0.6	14.4 ± 0.5	14.6 ± 0.4	14.5 ± 0.3
	$J_{20,3}$ (LMH)	12.8 ± 0.8	13.0 ± 0.8	13.2 ± 0.7	13.1 ± 0.6
$Flux_4$	$J_{T,4}$ (LMH)	18.6 ± 1.4	18.5 ± 1.5	18.5 ± 1.4	18.6 ± 1.5
	$J_{20,4}$ (LMH)	16.8 ± 1.0	16.7 ± 1.1	16.7 ± 1.1	16.7 ± 1.1

control method) on membrane permeability of AnMBRs. In the present study, the SGD step method consisted in progressively increasing/decreasing the SGD intensity for each flux. Firstly, the SGD was progressively increased from 0.25 to 2.0 $m^3\ m^{-2}\ h^{-1}$ following four SGD steps (0.25, 0.5, 1.0 and 2.0 $m^3\ m^{-2}\ h^{-1}$). Secondly, the SGD was progressively decreased from 2.0 to 0.25 $m^3\ m^{-2}\ h^{-1}$ following the same SGD steps. Each SGD step had a filtration duration of 15 min, whereas a relaxation period of 90 s was applied between steps. The permeate samples were obtained at the end of each SGD step. Permeate flow rate was measured three times per each SGD step to record the experimental flux. The liquor temperature was measured before starting each SGD step and all the fluxes were normalised to 20 °C by means of Eq. (1) (Wang et al., 2020):

$$J_T = J_{20} \cdot 1.025^{(T-20)} \quad (1)$$

where J_T is the measured flux (LMH), J_{20} is the normalised flux at 20 °C (LMH) and T is the sludge temperature (°C). The filtration resistance for distilled water and granular sludge filtration was determined by using Eq. (2). Subsequently, the filtration resistance caused by membrane fouling (R_F) was used as indicator to determine the extent of fouling for each condition (Eq. (3)).

$$R = \frac{TMP}{\mu_{20} \cdot J_{20}} \quad (2)$$

$$R_F = R_T - R_M \quad (3)$$

where R is the filtration resistance (m^{-1}), TMP is the transmembrane pressure (Pa), J_{20} is the normalised flux at 20 °C ($m^3\ m^{-2}\ s^{-1}$), μ_{20} is the water viscosity at 20 °C (Pa s), R_F is the foulant filtration resistance (m^{-1}), R_T is the total filtration resistance obtained during granular sludge filtration (m^{-1}) and R_M is the membrane resistance obtained during distilled water filtration (m^{-1}).

The short-term filtration tests for each flux and SGD were conducted in triplicate. The anaerobic granular sludge was replaced before each replicate to prevent substantial degradation of the soluble and colloidal compounds that could influence the membrane permeability and DCOM rejection of the system. All the replicates were carried out under similar solids concentration (Table S2 of the supplementary material). Error bars in figures represent the standard deviation.

2.4. Long-term filtration tests

Long-term filtration tests were conducted for four operational conditions: (1) J_{20} = 4.1 LMH and SGD = 0.5 $m^3\ m^{-2}\ h^{-1}$; (2) J_{20} = 7.8 LMH and SGD = 0.5 $m^3\ m^{-2}\ h^{-1}$; (3) J_{20} = 12.0 LMH and SGD = 1.0 $m^3\ m^{-2}\ h^{-1}$; and (4) J_{20} = 15.4 LMH and SGD = 1.0 $m^3\ m^{-2}\ h^{-1}$. These selected operational conditions represented the most favourable SGD for each membrane flux from the sort-term filtration tests (see Section 3.1).

The experimental cycle for the long-term filtration tests comprised four different stages: (1) distilled water filtration, (2) granular sludge filtration to determine the membrane permeability, (3) physical cleaning of the membrane with tap water and (4) chemical cleaning of the membrane with a 0.2% sodium hypochlorite solution for 4 h. These four stages were repeated for each of the four scenarios evaluated. It is worth mentioning that the duration of the chemical cleaning in the long-term filtration tests was longer than in the short-term tests since the extent of fouling is higher in the long-term trials. This intensive chemical cleaning protocol was applied to ensure the recovery of membrane permeability prior to the next filtration test. The determination of the permeability (Stage 2) comprised five filtration cycles of 45 min with a total duration of 225 min (5 × 45 min). A relaxation period of 90 s was applied between each filtration cycle. To obtain the experimental flux, the permeate flow rate was measured eight times per each filtration cycle. The liquor temperature was measured three times per each filtration cycle to record possible temperature variations during the experimental period. All the fluxes and membrane permeabilities were normalised to 20 °C (Eq. (1)). The normalised membrane permeability (K_{20}) at the end of the fifth cycle (225 min) was used for the economic analysis. The K_{20} was calculated by means of Eq. (4).

$$K_{20} = \frac{J_{20}}{TMP} \quad (4)$$

where K_{20} is the normalised permeability at 20 °C (LMH bar^{-1}), J_{20} is the normalised flux at 20 °C (LMH) and TMP is the transmembrane pressure (bar).

2.5. Analytical methods

TS and VS were measured following the Standard Method 2540G (APHA, 2017). The soluble total organic carbon (sTOC) analysis was conducted with a TOC analyser (Shimadzu, Japan). The soluble chemical oxygen demand (COD) was measured with COD LCK kits and an UV-VIS spectrophotometer (Hach Lange, Germany). The dissolved and colloidal fractions were obtained after filtering the samples with 1.2 μm filters (Whatman, UK). The pH was analysed with a pH electrode (VWR, USA). The zeta potential of the sludge samples was measured with a zeta potential analyser (Anton Paar, Spain). The particle size distribution of the initial granular sludge was obtained by sieving according to the method reported by Derlon et al. (2016).

Three-dimensional excitation-emission matrix fluorescence (3DEEM) was used to evaluate the membrane rejection of DCOM fluorophores. A Perkin-Elmer LS-55 spectrometer was used to obtain the fluorescence spectra for each sample. The samples were diluted with Milli-Q water by a factor of 150 to avoid overlapping signals. The emission and excitation spectra ranged from 280 to 600 nm and from 200 to 500 nm, respectively. Blank test with Milli-Q water was performed to normalise the spectra. The normalised spectra can be divided into different regions depending on the fluorophore analysed (Chen et al., 2003; Jacquin et al., 2018): (i) Region I + II, which corresponds to protein-like fluorophores; (ii) Region III, which corresponds to fulvic acid-like fluorophores; (iii) Region IV, which corresponds to soluble microbial product-like fluorophores and (iv) Region V, which corresponds to humic acid-like fluorophores. Further information on the methodology used for the 3DEEM analysis can be found in Jacquin et al. (2017).

2.6. Economic evaluation

2.6.1. Scenarios definition

The economic evaluation was conducted modelling a high-sized WWTP with a treatment capacity of 500,000 population equivalent (100,000 $m^3\ d^{-1}$). The WWTP was considered to have a mainstream granular AnMBR system for sewage treatment. Detailed information of the different scenarios and conditions considered for the economic analysis can be found in Table S3 of the supplementary material.

The economic analysis evaluated the four scenarios selected for the long-term filtration tests. Scenario 1: J_{20} = 4.1 LMH and SGD = 0.5 $m^3\ m^{-2}\ h^{-1}$; Scenario 2: J_{20} = 7.8 LMH and SGD = 0.5 $m^3\ m^{-2}\ h^{-1}$; Scenario 3: J_{20} = 12.0 LMH and SGD = 1.0 $m^3\ m^{-2}\ h^{-1}$; and Scenario 4: J_{20} = 15.4 LMH and SGD = 1.0 $m^3\ m^{-2}\ h^{-1}$.

Three different chemical cleaning conditions were considered for each scenario. Condition A: clean in place (CIP) and clean out of place (COP) performed 52 and 2 times per year, respectively; Condition B: CIP and COP performed 26 and 1 times per year, respectively; and Condition C: CIP and COP performed 104 and 3 times per year, respectively. Further information on chemical cleaning protocol selection can be found in Section 2.6.2.

2.6.2. Cost calculation

Capital and operating costs for the granular AnMBR system were included in the economic analysis. The capital costs accounted for membrane and blower purchase costs. The operating costs accounted for energy

consumption for gas sparging and permeate pumping, membrane replacement cost and chemical reagents cost. It is worth mentioning that all the costs and revenue that were not influenced by flux and SGD (e.g. capital cost for bioreactor construction, methane production) have not been included in this economic evaluation since they would be similar regardless of the flux and SGD applied. Detailed information of the parameters used for cost calculations can be found in Table S4 of the supplementary material.

The capital costs for membranes and blowers were considered to be 50 € m^{-2} and 4.15 € Nm^{-3} h, respectively (Verrecht et al., 2010; Vinardell et al., 2021). The required power of the blower for gas sparging was calculated by means of Eq. (5) (Pretel et al., 2014):

$$P_B = \frac{M \cdot R \cdot T}{(\alpha-1)\cdot \eta_B} \cdot \left[\left(\frac{P_2}{P_1}\right)^{\frac{\alpha-1}{\alpha}} - 1\right] \quad (5)$$

where P_B is the power of the blower (W), M is the biogas molar flow rate (mol s^{-1}), T is the temperature of the biogas (°K), R is the ideal gas constant (J mol^{-1} K^{-1}), η_B is the blower efficiency (0.80), α is the adiabatic coefficient, P_1 is the absolute pressure in the inlet side of the blower (atm) and P_2 is the absolute pressure in the impulsion side of the blower (atm).

Eq. (6) was used to obtain the required power for the permeate pump (Pretel et al., 2014):

$$P_{PP} = \frac{TMP \cdot Q_P}{\eta_{PP}} \quad (6)$$

where P_{PP} is the power of the permeate pump (W), Q_P is the permeate flow rate (m^3 s^{-1}), TMP is transmembrane pressure (Pa) and η_{pp} is the permeate pump efficiency (0.85).

Chemical cleaning requirements depend on the extent of membrane fouling in the AnMBR (Wang et al., 2014). This means that those scenarios with a higher membrane permeability and lower membrane fouling would require a less intensive chemical cleaning. In the present study, the concentration of chemical reagents for the economic analysis was defined considering the membrane permeability of each scenario, obtained from the long-term filtration tests. Scenario 4 was considered the reference scenario from which the concentration of chemical reagents was calculated for the other three scenarios. Scenario 4 was the reference since Scenario 4 features a similar flux (J_T = 17.9 LMH) than typical fluxes for full-scale aerobic MBR plants (Judd, 2010; Verrecht et al., 2010). Therefore, it was considered that typical chemical cleaning protocols reported in the literature for full-scale MBR plants could be extendible to Scenario 4.

The chemical cleaning protocol for Scenario 4 was adapted from Brepols et al. (2008). The chemical cleaning included both CIP and COP protocols. The CIP protocol was assumed to be performed once a week (52 times per year) with a 0.05% sodium hypochlorite solution and a 2000 mg L^{-1} citric acid solution. The COP protocol was assumed to be performed twice a year with a 0.1% sodium hypochlorite solution and a 2000 mg L^{-1} citric acid solution (Condition A). The volume of chemicals was considered to be 17.5 L m^{-2} (Ramos et al., 2014). Subsequently, the consumption of chemical reagents for Scenario 1, 2 and 3 was calculated considering that the consumption of chemical reagents was inversely proportional to the membrane permeability. Specifically, the ratio between normalised permeability of the Scenario and normalised permeability of the reference Scenario 4 ($K_{20,x}/K_{20,4}$) was used to calculate the amount of chemical reagents required for each scenario. The duration of the CIP and COP for each chemical reagent was 2 and 16 h, respectively. To evaluate the impact of chemical cleaning protocol frequency on operating costs, two other cleaning frequencies were considered. Condition B: CIP and COP performed 26 and 1 times per year, respectively; and Condition C: CIP and COP performed 104 and 3 times per year, respectively.

The extent of chemical cleaning also has an impact on membrane replacement cost since chemical cleaning reduces the lifetime of the membranes. The membrane replacement cost was calculated considering that the membranes had to be replaced when the maximum cumulative chlorine contact of 500,000 mg L^{-1}-h was exceeded (Robles et al., 2014). The residual economic value of the membranes at the end of the plant lifetime was included in the economic evaluation.

The capital expenditures (CAPEX) and operating expenditures (OPEX) for the different scenarios and conditions were calculated and Eq. (7) was used to obtain the discounted lifetime cost (DLC) for each scenario:

$$DLC = CAPEX + \sum_{t=1}^{T} \frac{OPEX_t}{(1+i)^t} \quad (7)$$

where CAPEX is the capital expenditure (€), $OPEX_t$ is the OPEX at year t (€), i is the discount rate (5%) and T is the plant lifetime (20 years).

3. Results and discussion

3.1. Effect of flux and SGD on membrane filtration resistance

Fig. 2 shows the R_F of the short-term filtration tests for the different fluxes and SGDs. The results show that the extent of membrane fouling was clearly influenced by the SGD intensity since the R_F decreased as the SGD increased. Higher fluxes increased the extent of membrane fouling, which made it necessary to substantially increase SGD intensities to reduce R_F values. Regarding $Flux_1$ and $Flux_2$ (J_T and J_{20} < 10 LMH), a reduction of R_F was observed when the SGD increased from 0.25 to 0.5 m^3 m^{-2} h^{-1}. However, when the SGD was further increased the R_F reduction was minimal. These results show that a SGD of 0.5 m^3 m^{-2} h^{-1} was the most favourable condition for membrane fouling control when the membrane was operated below 10 LMH (Fig. 2). Regarding $Flux_3$ and $Flux_4$ (J_T and J_{20} > 10 LMH), a noticeable reduction of R_F was observed as the SGD increased from 0.25 to 2.0 m^3 m^{-2} h^{-1}. However, the R_F reduction was progressively less pronounced as the SGD increased. This was particularly important when the SGD increased from 1.0 to 2.0 m^3 m^{-2} h^{-1} since this SGD step only provided a relatively moderate R_F reduction at expenses of doubling the gas sparging demand. Accordingly, it is conceivable to state that a SGD of 1.0 m^3 m^{-2} h^{-1} was the most favourable condition for membrane fouling control when the membrane was operated above 10 LMH. These results align with other AnMBR studies that reported that SGDs above 1.0 m^3 m^{-2} h^{-1} did not lead to substantial improvements in membrane fouling control (Ruigómez et al., 2016; Wang et al., 2018).

These results suggest that the extent of membrane fouling was substantially higher when the membrane was operated at fluxes above 10 LMH. The R_F was higher for $Flux_3$ and $Flux_4$ (J_T and J_{20} > 10 LMH) than for $Flux_1$ and $Flux_2$ (J_T and J_{20} < 10 LMH) regardless of the SGD condition applied. These results also highlight that, besides the SGD, it is important to include the impact of flux on fouling extent since the best strategy for fouling control requires a compromise solution considering flux, SGD intensity and fouling extent.

3.2. Effect of flux and SGD on dissolved and colloidal organic matter rejection

Fig. 3 shows the sCOD membrane rejection for the different fluxes and SGDs evaluated, where sCOD rejection results have been grouped for each flux and SGD condition. The specific sCOD membrane rejection for each condition is shown in Fig. S1 of the supplementary material. The sCOD rejection ranged between 31 and 44% for the different conditions (Fig. 3). The capacity of the ultrafiltration/microfiltration membranes to reject DCOM can be attributed to the pore size exclusion phenomenon or chemical/physical interactions of the soluble compounds with the membrane and/or the fouling layer formed on its surface (Jacquin et al., 2018; Liu et al., 2021; Xin et al., 2020). The results show no direct correlation between the SGD/flux and the rejection of sCOD. Regarding the SGD, the sCOD rejection was similar (33–38%) regardless of the SGD applied and no significant differences were observed between the four SGD conditions ($p > 0.05$). Regarding the flux, the sCOD rejection was similar for $Flux_1$, $Flux_2$ and $Flux_3$ (31–35%) and no significant differences were observed between them ($p > 0.05$). Conversely, $Flux_4$ featured a statistically

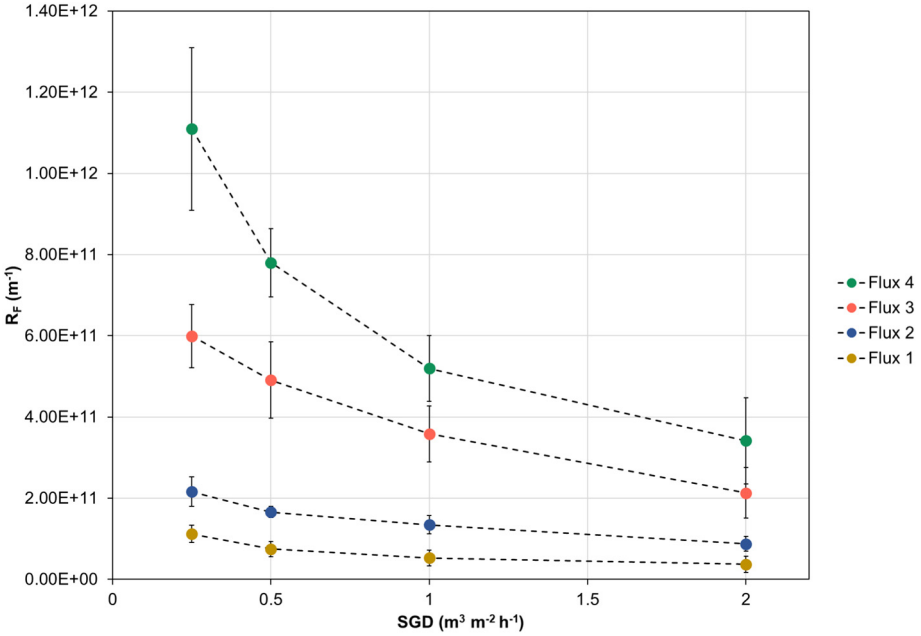

Fig. 2. R_F for the four SGD and fluxes evaluated. Error bars represent standard deviations (n = 6). $Flux_1$ = 4.4 LMH; $Flux_2$ = 8.7 LMH; $Flux_3$ = 13.0 LMH; $Flux_4$ = 16.7 LMH.

significantly higher sCOD rejection (44%) when compared to the other flux conditions ($p < 0.05$). These differences could be attributed to changes in the concentration and composition of DCOM. The fluorescence intensity of the mixed liquor samples was higher for $Flux_4$ than for $Flux_1$, $Flux_2$ and $Flux_3$, which was particularly noticeable for Region I + II of the 3DEEM spectra (see Fig. S2 of the supplementary material). It is hypothesised that the higher sCOD rejection achieved in $Flux_4$ could be attributed to the higher content of DCOM in Region I + II since the DCOM compounds contained in this region are more retained by the membrane (see Table 2).

Table 2 shows the membrane rejection of fluorophores DCOM for the different regions of the 3DEEM spectra. The rejection of fluorophores DCOM ranged between 34 and 44%, which was similar to the sCOD rejection. Table 2 also shows that membrane rejected between 39 and 50% of the fluorophores DCOM of Region I + II. The higher rejection of fluorophores DCOM in Region I + II (protein-like fluorophores) in comparison to the other regions can be mainly attributed to the high molecular weight and hydrophilic nature of proteins (Jacquin et al., 2018; Xin et al., 2020). This is particularly important since Region I + II was predominant in the 3DEEM spectra (67–79%), followed by Region III + V (17–29%) and Region IV (2–4%) (see Fig. S3 and Table S5 of the supplementary material). Considering the predominance of protein-like fluorophores in the 3DEEM spectra and that these fluorophores are more retained by the membrane, it is stated that proteins could play an important role in membrane fouling of anaerobic granular sludge filtration. Finally, it is worth mentioning that the results of Table 2 corroborate that flux and SGD conditions did not feature a direct correlation with the DCOM rejection. However, experiments

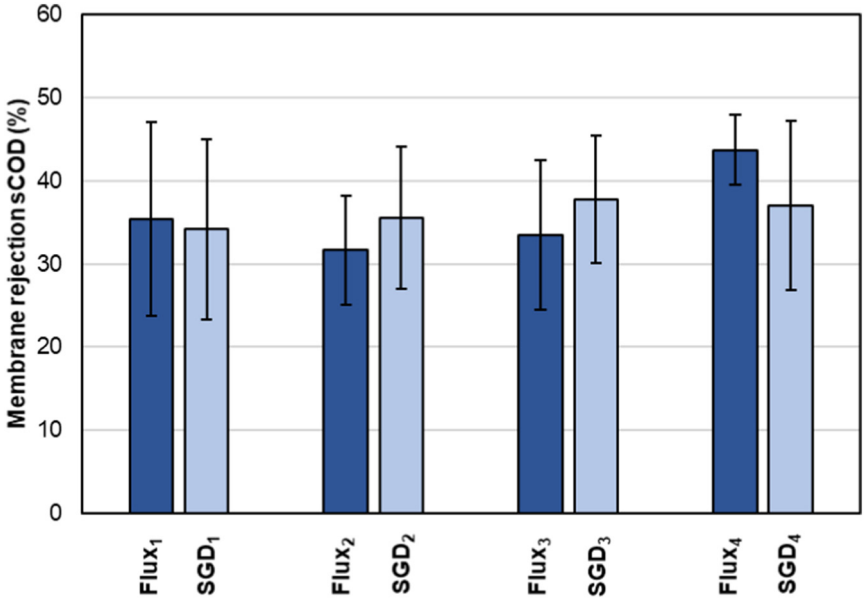

Fig. 3. Membrane rejection of sCOD for the four SGD and fluxes evaluated. Error bars represent standard deviations (n = 12). $Flux_1$ = 4.4 LMH; $Flux_2$ = 8.7 LMH; $Flux_3$ = 13.0 LMH; $Flux_4$ = 16.7 LMH; SGD_1 = 0.25 m^3 m^{-2} h^{-1}; SGD_2 = 0.50 m^3 m^{-2} h^{-1}; SGD_3 = 1.0 m^3 m^{-2} h^{-1}; SGD_4 = 2.0 m^3 m^{-2} h^{-1}.

Table 2
Membrane rejection of the fluorophores DCOM compounds for the different regions of the 3DEEM spectra. Errors represent standard deviations (n = 4). $Flux_1$ = 4.4 LMH; $Flux_2$ = 8.7 LMH; $Flux_3$ = 13.0 LMH; $Flux_4$ = 16.7 LMH; SGD_1 = 0.25 $m^3\ m^{-2}\ h^{-1}$; SGD_2 = 0.50 $m^3\ m^{-2}\ h^{-1}$; SGD_3 = 1.0 $m^3\ m^{-2}\ h^{-1}$; SGD_4 = 2.0 $m^3\ m^{-2}\ h^{-1}$.

	$Flux_1$	$Flux_2$	$Flux_3$	$Flux_4$	SGD_1	SGD_2	SGD_3	SGD_4
Rejection region I + II (%)	45.2 ± 6.8	44.3 ± 3.1	39.1 ± 10.9	50.2 ± 6.3	40.2 ± 10.0	48.5 ± 4.7	43.9 ± 4.9	46.7 ± 10.7
Rejection region IV (%)	47.2 ± 8.5	26.4 ± 3.4	26.3 ± 8.3	39.8 ± 4.6	34.6 ± 10.6	38.2 ± 12.9	28.1 ± 8.8	43.0 ± 4.4
Rejection region III + V (%)	16.1 ± 12.6	18.1 ± 3.8	23.1 ± 9.1	18.8 ± 6.8	13.7 ± 5.6	26.2 ± 4.6	15.8 ± 6.4	21.3 ± 13.5
Total Rejection (%)	40.2 ± 7.6	38.6 ± 2.2	34.8 ± 9.9	43.7 ± 5.9	34.8 ± 8.9	43.6 ± 4.6	37.9 ± 4.4	41.7 ± 9.7

with a longer filtration duration are necessary to evaluate the impact that the formation and consolidation of a gel or cake layer on the membrane surface have on the DCOM rejection.

3.3. Long-term filtration tests

Table 3 shows the experimental flux, K_{20} and $K_{20,x}/K_{20,4}$ ratio obtained from the long-term filtration tests. The results show that K_{20} increased as the flux decreased, which aligns with the short-term filtration tests since the K_{20} was higher at lower fluxes. This reinforces the idea that studies evaluating the SGD intensity should also consider the impact of flux since this parameter plays a key role in membrane fouling extent. The K_{20} progressively decreased over time and, except for Scenario 1, reached relatively constant values after about 135 min (see Fig. S4 of the supplementary material). Table 3 also shows that K_{20} was eight and four times higher in Scenario 1 (J_{20} = 4.1 LMH) and Scenario 2 (J_{20} = 7.8 LMH) than in Scenario 4 (J_{20} = 15.4 LMH), respectively. These results highlight that it is important to evaluate if the higher operating costs required for membrane fouling control could offset the lower costs associated with membrane purchasing when the membrane system is operated at higher fluxes.

3.4. Effect of flux and SGD on process economics

3.4.1. Discounted lifetime cost for the different scenarios and conditions

Fig. 4 shows the DLC for the four scenarios and the three chemical cleaning conditions under study. Detailed information of each scenario and chemical cleaning condition can be found in Table S3. The results show that energy consumption for gas sparging was the most important cost contributor for all the scenarios, representing between 35 and 73% of the DLC. Scenario 1 consumed a higher amount of energy for gas sparging than Scenario 3 and 4, although Scenario 1 required a lower SGD (0.5 $m^3\ m^{-2}\ h^{-1}$) than Scenario 3 and 4 (1.0 $m^3\ m^{-2}\ h^{-1}$). This is due to the higher membrane area (lower flux) of Scenario 1 that increased the total energy required for gas sparging, despite requiring a lower SGD.

The results of Fig. 4 also show that membrane purchasing cost represented an important fraction of the DLC, but its contribution decreased from 33–35 to 10–19% as the flux increased from 4.1 to 15.4 LMH, respectively. Chemical and membrane replacement costs also had an impact on DLC, particularly in Scenario 4 (J_{20} = 15.4 LMH), where the higher flux required more intensive chemical cleaning to reduce the extent of fouling. In Scenario 4, the membrane replacement cost and chemical cleaning represented 8.5–34.6 and 8.1–18.2% of the DLC, respectively. The increase of chemical cleaning requirements was accompanied by a reduction of the membrane lifetime, which increased the membrane replacement cost. The contribution of blower purchase cost and energy consumption for permeate pumping can be considered negligible since they did not account for more than 2% of the DLC in any of the scenarios and conditions evaluated.

Fig. 4 also illustrates that Scenario 2 was the most competitive scenario for chemical cleaning Condition A and C, whereas Scenario 4 was the most competitive scenario for chemical cleaning Condition B. These results highlight that the chemical cleaning strategy had a direct impact on the economic prospect of AnMBR systems. The impact of the chemical cleaning strategy on DLC was higher in Scenario 4 since this scenario featured the highest consumption of chemicals because of its lower membrane permeability. For this reason, Scenario 4 was the most economical scenario for chemical cleaning condition B since the lower frequency of CIP and COP in Condition B led to a noticeable reduction of the DLC when compared with Condition A and C (Fig. 4). However, Condition B considered that the frequency of CIP and COP would be lower than typical chemical cleaning frequencies reported for aerobic MBR systems. However, this consideration is unlikely to occur in an AnMBR, particularly considering that membrane fouling is generally higher under anaerobic than under aerobic conditions (Yao et al., 2020). Therefore, it is expected that similar (Condition A) or even higher (Condition C) chemical cleaning frequencies in comparison to aerobic MBR systems would be required in future full-scale AnMBR systems. Scenario 2 was the less costly scenario in Condition A and C, followed by Scenario 3 and 4. The DLC difference between these scenarios was higher for Condition C than for Condition A since Condition C considered a higher frequency of CIP and COP than Condition A.

These results show that Scenario 2 is the most favourable scenario. This indicates that operating the membrane system under moderate fluxes (J_{20} = 7.8 LMH) and SGDs (0.5 $m^3\ m^{-2}\ h^{-1}$) could be the most favourable strategy for membrane fouling control in the granular AnMBR system. Finally, it is worth mentioning that Scenario 1 featured the highest DLC regardless of the chemical cleaning condition applied, which shows that operating the membrane system at fluxes below 5 LMH is not a feasible option.

3.4.2. Sensitivity analysis

Fig. 5 shows the sensitivity analysis of the DLC for a ±30% variation of the most important economic parameters. The sensitivity analysis was carried out for Condition A since this was considered the most representative condition for the chemical cleaning. The results show that electricity price variation had the highest impact on DLC since an increase or decrease of this parameter substantially affected the energy cost for gas sparging. Membrane cost variation featured the second highest impact on DLC. These results illustrate that lower electricity and membrane costs through improvements in SGD and membrane permeability are crucial to improve the competitiveness of granular AnMBR systems. The DLC variation caused by membrane cost in Scenario 4 was 20 and 34% higher than in Scenario 2 and 3, respectively, although Scenario 4 required a lower membrane area than Scenario 2 and 3 (Fig. 5). The higher impact of membrane cost for Scenario 4 can be attributed to the higher membrane replacement cost in this scenario. These results highlight that the variation of the membrane cost does not only affect the initial membrane purchasing cost, but also the cost required to replace the membranes during the plant lifetime. The parameters associated with the chemical cleaning strategy (i.e. chemical reagents price, chemical cleaning concentration and CIP frequency) increased their impact on DLC as the flux increased (higher membrane fouling). As shown in Fig. 4, the variation of chemical cleaning strategy affected

Table 3
Summary of the results obtained in the long-term filtration tests. Fig. S4 shows the evolution of membrane permeability over time. Errors represent standard deviations (n = 40).

	SGD ($m^3\ m^{-2}\ h^{-1}$)	J_T (LMH)	J_{20} (LMH)	$K_{20,t=225}$ (LMH bar^{-1})	$K_{20,x}/K_{20,4}$
Scenario 1	0.5	4.7 ± 0.1	4.1 ± 0.1	1175	8.8
Scenario 2	0.5	9.2 ± 0.1	7.8 ± 0.1	506	3.8
Scenario 3	1.0	13.7 ± 0.1	12.0 ± 0.1	315	2.4
Scenario 4	1.0	17.9 ± 0.3	15.4 ± 0.1	133	1.0

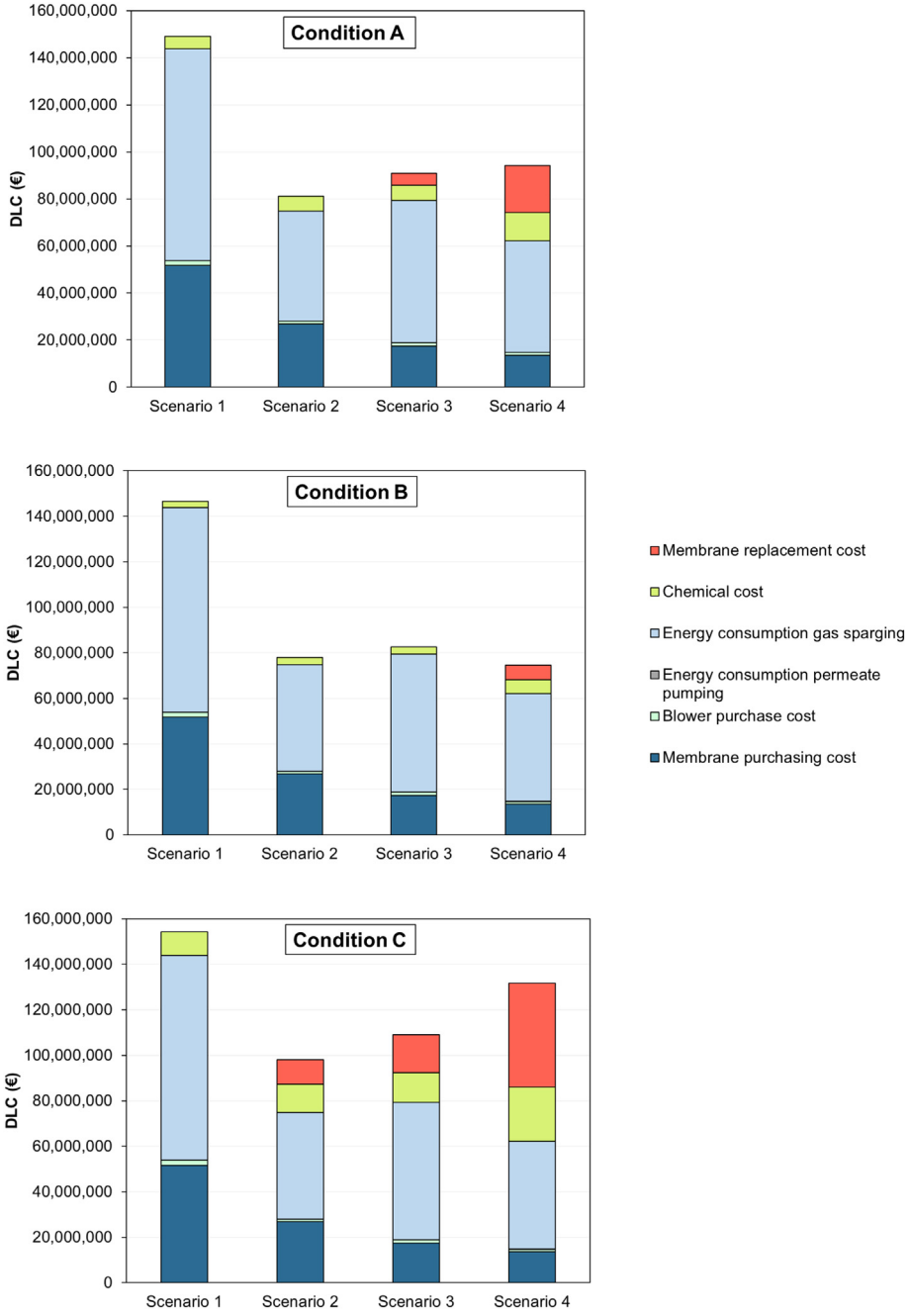

Fig. 4. Discounted lifetime cost (DLC) for the four scenarios and three chemical cleaning conditions evaluated. Table S3 shows detailed information of each scenario and chemical cleaning condition.

the amount of chemicals purchased as well as the durability of the membranes. Therefore, these results show the importance of selecting an optimum strategy for chemical cleaning, particularly in those scenarios that require more chemicals to control irreversible membrane fouling.

Fig. 6 shows the sensitivity analysis of the DLC for a variation of the $K_{20,x}/K_{20,4}$ ratio in Scenario 1, 2 and 3. This sensitivity analysis was performed to evaluate how possible variations of the $K_{20,x}/K_{20,4}$ ratio could affect the economic prospect of each scenario. The results illustrate that the DLC sharply decreased as the $K_{20,x}/K_{20,4}$ ratio increased from 1 to 4. This is because the increase in membrane permeability decreases the consumption of chemical reagents with a direct impact on membrane durability. However, only marginal reductions of DLC were obtained when the $K_{20,x}/K_{20,4}$ ratio was above 4, which suggests that the contribution of chemical cleaning and membrane replacement to the DLC substantially decreased as the $K_{20,x}/K_{20,4}$ ratio increased. Scenario 2 and Scenario 3 were more competitive than Scenario 4 when the $K_{20,x}/K_{20,4}$ ratio was above 2.5 and 2.0, respectively. Fig. 6 also shows that Scenario 2 slightly outcompeted Scenario 3 when the $K_{20,x}/K_{20,4}$ ratio was above 3. This illustrates that Scenario 2 is more economical than Scenario 3 since (i) the membrane permeability of Scenario 2 was higher than Scenario 3 since it was operated at a lower flux and (ii) an experimental $K_{20,x}/K_{20,4}$ ratio of 3.8 (>3) was obtained for Scenario 2 in the long term-tests (see Table 3). Finally, it is worth mentioning that Scenario 1 was not economically favourable regardless of the $K_{20,x}/K_{20,4}$ ratio, which reinforces the idea that AnMBR operation at low fluxes is not economically feasible.

4. Conclusions

The results of this study showed that the extent of membrane fouling is clearly influenced by membrane flux and SGD conditions. The most

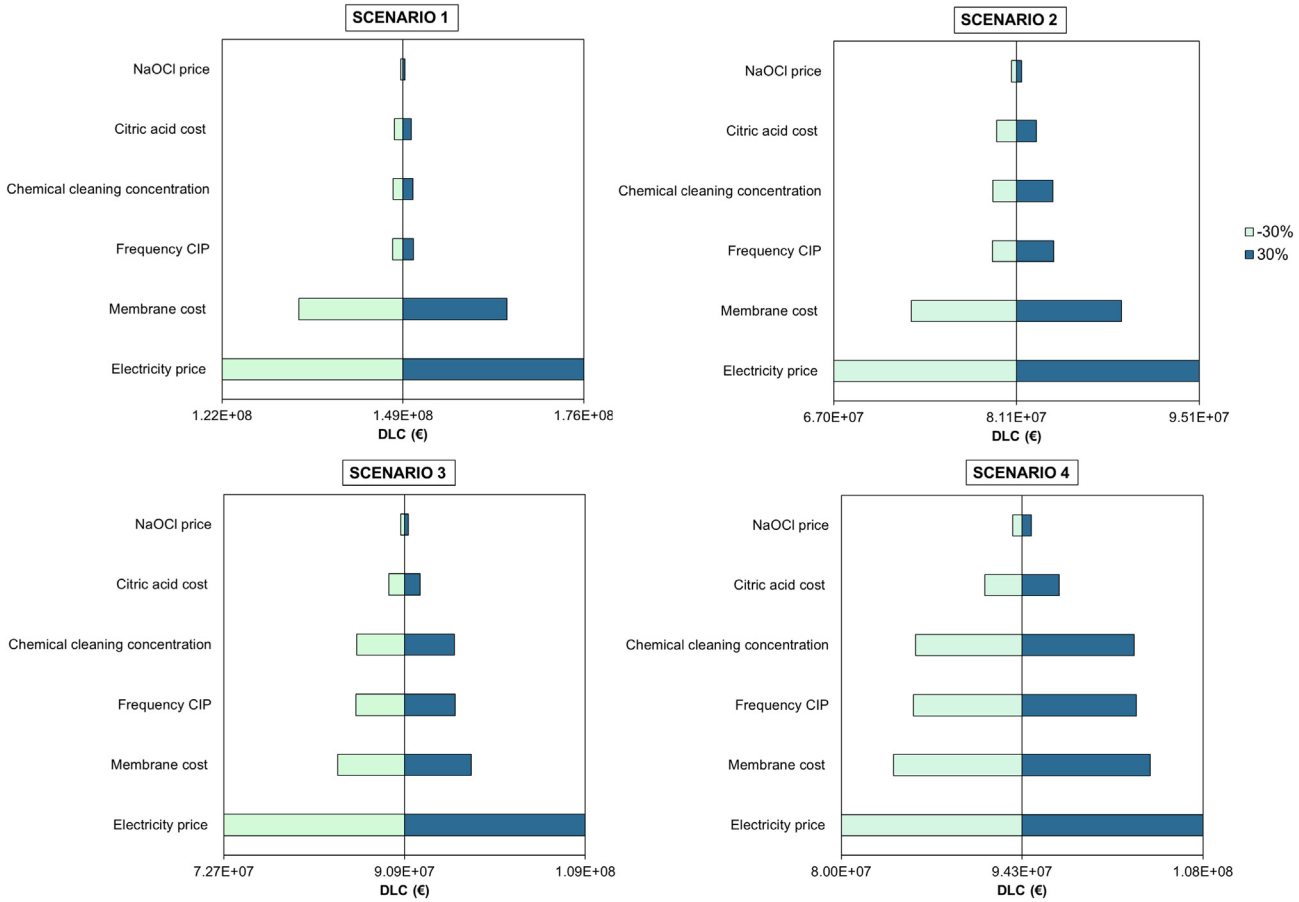

Fig. 5. Sensitivity analysis of the discounted lifetime cost (DLC) for a ± 30% variation of the most important economic parameters for the four scenarios. The sensitivity analysis was carried out for chemical cleaning Condition A.

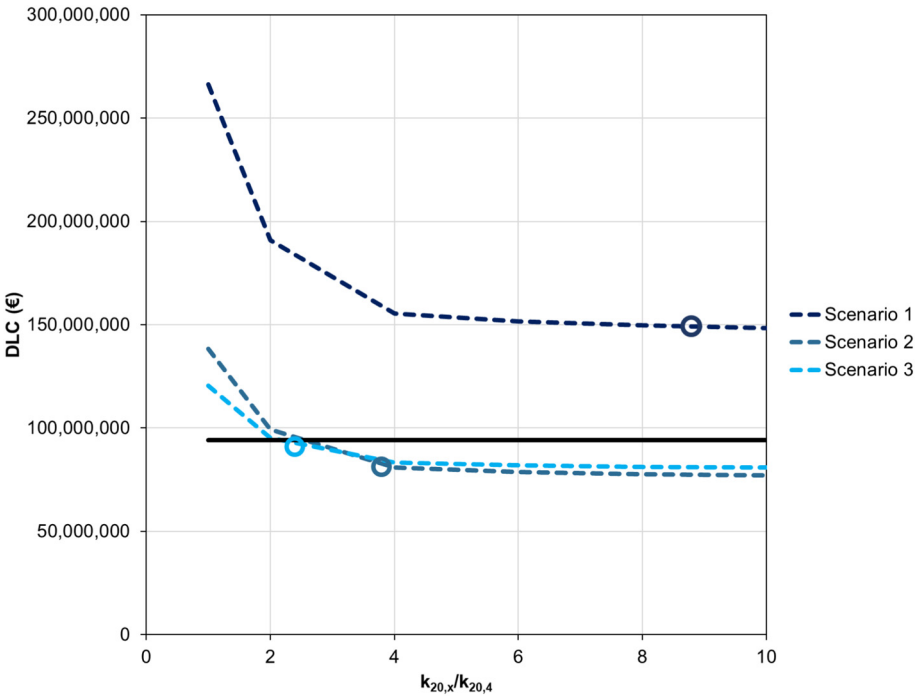

Fig. 6. Sensitivity analysis of the discounted lifetime cost (DLC) variation for Scenario 1, 2 and 3 in function to the $K_{20,x}/K_{20,4}$ ratio. The horizontal black bar represents the DLC of Scenario 4 that remains constant because this is the reference scenario. The circles indicate the experimental $K_{20,x}/K_{20,4}$ ratio. The sensitivity analysis was carried out for chemical cleaning Condition A.

favourable SGD condition was 0.5 $m^3\ m^{-2}\ h^{-1}$ at J_{20} of 4.4 and 8.7 LMH, whereas the most favourable SGD condition was 1.0 $m^3\ m^{-2}\ h^{-1}$ at J_{20} of 13.0 and 16.7 LMH. The results also showed that a suitable SGD needs to consider both gas sparging rate and membrane flux. The membrane rejection of DCOM was between 31 and 44%. No direct correlation between flux/SGD conditions and DCOM rejection was observed. The protein-like fluorophores were predominant (67–79%) in both mixed liquor and permeate samples and were relatively high retained by the membrane (39–50%). This suggests that protein-like fluorophores could play an important role in membrane fouling. The economic analysis indicated that operating the membrane at moderate fluxes (J_{20} = 7.8 LMH) and SGDs (0.5 $m^3\ m^{-2}\ h^{-1}$) is the most favourable strategy for granular AnMBR systems. Finally, a sensitivity analysis illustrated that electricity and membrane cost have the highest impact on DLC, which highlights the importance of reducing SGD requirements and enhancing membrane permeability to improve the competitiveness of granular AnMBRs.

CRediT authorship contribution statement

Sergi Vinardell: Conceptualization, Methodology, Formal analysis, Investigation, Data curation, Writing – original draft, Writing – review & editing, Visualization. **Lucie Sanchez:** Methodology, Writing – review & editing, Visualization. **Sergi Astals:** Writing – review & editing, Supervision. **Joan Mata-Alvarez:** Writing – review & editing, Supervision. **Joan Dosta:** Writing – review & editing, Supervision. **Marc Heran:** Writing – review & editing, Supervision, Funding acquisition. **Geoffroy Lesage:** Conceptualization, Methodology, Writing – review & editing, Supervision, Funding acquisition.

Declaration of competing interest

The authors declare that they have no known competing financial interests or personal relationships that could have appeared to influence the work reported in this paper.

Acknowledgments

This work was supported by a grant overseen by the French National Research Agency (ANR) as part of the “JCJC” program BàMAn (ANR-18-CE04-0001-01). Sergi Vinardell is grateful to the Generalitat de Catalunya for his predoctoral FI grant and the travel stipend (2019 FI_B 00394). Sergi Astals is grateful to the Spanish Ministry of Science and Innovation for his Ramon y Cajal fellowship (RYC-2017-22372).

Appendix A. Supplementary data

Supplementary data to this article can be found online at https://doi.org/10.1016/j.scitotenv.2022.153907.

References

Anjum, F., Khan, I.M., Kim, J., Aslam, M., Blandin, G., Heran, M., Lesage, G., 2021. Trends and progress in AnMBR for domestic wastewater treatment and their impacts on process efficiency and membrane fouling. Environ. Technol. Innov. 21, 101204.

APHA, 2017. Standard Methods for the Examination of Water and Wastewater. Federation. Water Environmental American Public Health Association (APHA), Washington, USA.

Aslam, M., Charfi, A., Lesage, G., Heran, M., Kim, J., 2017. Membrane bioreactors for wastewater treatment: a review of mechanical cleaning by scouring agents to control membrane fouling. Chem. Eng. J. 307, 897–913.

Brepols, C., Drensla, K., Janot, A., Trimborn, M., Engelhardt, N., 2008. Strategies for chemical cleaning in large scale membrane bioreactors. Water Sci. Technol. 57, 457–463.

Chen, C., Guo, W., Ngo, H.H., 2016. Advances in granular growth anaerobic membrane bioreactor (G-AnMBR) for low strength wastewater treatment. J. Energy Environ. Sustain. 1, 77–83.

Chen, C., Guo, W., Ngo, H.H., Chang, S.W., Duc Nguyen, D., Dan Nguyen, P., Bui, X.T., Wu, Y., 2017. Impact of reactor configurations on the performance of a granular anaerobic membrane bioreactor for municipal wastewater treatment. Int. Biodeterior. Biodegrad. 121, 131–138.

Chen, W., Westerhoff, P., Leenheer, J.A., Booksh, K., 2003. Fluorescence excitation-emission matrix regional integration to quantify spectra for dissolved organic matter. Environ. Sci. Technol. 37, 5701–5710.

De Vela, R.J., 2021. A review of the factors affecting the performance of anaerobic membrane bioreactor and strategies to control membrane fouling. Rev. Environ. Sci. Biotechnol. 20, 607–644.

Dereli, R.K., Ersahin, M.E., Ozgun, H., Ozturk, I., Jeison, D., van der Zee, F., van Lier, J.B., 2012. Potentials of anaerobic membrane bioreactors to overcome treatment limitations induced by industrial wastewaters. Bioresour. Technol. 122, 160–170.

Derlon, N., Wagner, J., da Costa, R.H.R., Morgenroth, E., 2016. Formation of aerobic granules for the treatment of real and low-strength municipal wastewater using a sequencing batch reactor operated at constant volume. Water Res. 105, 341–350.

Dong, Q., Parker, W., Dagnew, M., 2016. Long term performance of membranes in an anaerobic membrane bioreactor treating municipal wastewater. Chemosphere 144, 249–256.

Fox, R.A., Stuckey, D.C., 2015. The effect of sparging rate on transmembrane pressure and critical flux in an AnMBR. J. Environ. Manag. 151, 280–285.

Gouveia, J., Plaza, F., Garralon, G., Fdz-Polanco, F., Peña, M., 2015a. A novel configuration for an anaerobic submerged membrane bioreactor (AnSMBR). Long-term treatment of municipal wastewater under psychrophilic conditions. Bioresour. Technol. 198, 510–519.

Gouveia, J., Plaza, F., Garralon, G., Fdz-Polanco, F., Peña, M., 2015b. Long-term operation of a pilot scale anaerobic membrane bioreactor (AnMBR) for the treatment of municipal wastewater under psychrophilic conditions. Bioresour. Technol. 185, 225–233.

Jacquin, C., Lesage, G., Traber, J., Pronk, W., Heran, M., 2017. Three-dimensional excitation and emission matrix fluorescence (3DEEM) for quick and pseudo-quantitative determination of protein- and humic-like substances in full-scale membrane bioreactor (MBR). Water Res. 118, 82–92.

Jacquin, C., Teychene, B., Lemee, L., Lesage, G., Heran, M., 2018. Characteristics and fouling behaviors of dissolved organic matter fractions in a full-scale submerged membrane bioreactor for municipal wastewater treatment. Biochem. Eng. J. 132, 169–181.

Ji, J., Chen, Y., Hu, Y., Ohtsu, A., Ni, J., Li, Y., Sakuma, S., Hojo, T., Chen, R., Li, Y.Y., 2021. One-year operation of a 20-L submerged anaerobic membrane bioreactor for real domestic wastewater treatment at room temperature: pursuing the optimal HRT and sustainable flux. Sci. Total Environ. 775, 145799.

Judd, S., 2010. The MBR Book: Principles and Applications of Membrane Bioreactors for Water and Wastewater Treatment. Butterworth-Heinemann, Oxford.

Krzeminski, P., Leverette, L., Malamis, S., Katsou, E., 2017. Membrane bioreactors – a review on recent developments in energy reduction, fouling control, novel configurations, LCA and market prospects. J. Memb. Sci. 527, 207–227.

Le Clech, P., Jefferson, B., Chang, I.S., Judd, S.J., 2003. Critical flux determination by the flux-step method in a submerged membrane bioreactor. J. Membr. Sci. 227, 81–93.

Liu, J., Zhao, M., Duan, C., Yue, P., Li, T., 2021. Removal characteristics of dissolved organic matter and membrane fouling in ultrafiltration and reverse osmosis membrane combined processes treating the secondary effluent of wastewater treatment plant. Water Sci. Technol. 83, 689–700.

Maaz, M., Yasin, M., Aslam, M., Kumar, G., Atabani, A.E., Idrees, M., Anjum, F., Jamil, F., Ahmad, R., Khan, A.L., Lesage, G., Heran, M., Kim, J., 2019. Anaerobic membrane bioreactors for wastewater treatment: novel configurations, fouling control and energy considerations. Bioresour. Technol. 283, 358–372.

Martin-Garcia, I., Monsalvo, V., Pidou, M., Le-Clech, P., Judd, S.J., McAdam, E.J., Jefferson, B., 2011. Impact of membrane configuration on fouling in anaerobic membrane bioreactors. J. Membr. Sci. 382, 41–49.

McCarty, P.L., Bae, J., Kim, J., 2011. Domestic wastewater treatment as a net energy producer - can this be achieved? Environ. Sci. Technol. 45, 7100–7106.

Meng, F., Zhang, S., Oh, Y., Zhou, Z., Shin, H.S., Chae, S.R., 2017. Fouling in membrane bioreactors: an updated review. Water Res. 114, 151–180.

Odriozola, M., Lousada-Ferreira, M., Spanjers, H., van Lier, J.B., 2021. Effect of sludge characteristics on optimal required dosage of flux enhancer in anaerobic membrane bioreactors. J. Membr. Sci. 619, 118776.

Ozgun, H., Dereli, R.K., Ersahin, M.E., Kinaci, C., Spanjers, H., Van Lier, J.B., 2013. A review of anaerobic membrane bioreactors for municipal wastewater treatment: integration options, limitations and expectations. Sep. Purif. Technol. 118, 89–104.

Pretel, R., Robles, A., Ruano, M.V., Seco, A., Ferrer, J., 2014. The operating cost of an anaerobic membrane bioreactor (AnMBR) treating sulphate-rich urban wastewater. Sep. Purif. Technol. 126, 30–38.

Ramos, C., Zecchino, F., Ezquerra, D., Diez, V., 2014. Chemical cleaning of membranes from an anaerobic membrane bioreactor treating food industry wastewater. J. Memb. Sci. 458, 179–188.

Robles, A., Ruano, M.V., Ribes, J., Seco, A., Ferrer, J., 2014. Model-based automatic tuning of a filtration control system for submerged anaerobic membrane bioreactors (AnMBR). J. Memb. Sci. 465, 14–26.

Robles, A., Ruano, M.V., Ribes, J., Ferrer, J., 2013. Factors that affect the permeability of commercial hollow-fibre membranes in a submerged anaerobic MBR (HF-SAnMBR) system. Water Res. 47, 1277–1288.

Ruigómez, I., Vera, L., González, E., González, G., Rodríguez-Sevilla, J., 2016. A novel rotating HF membrane to control fouling on anaerobic membrane bioreactors treating wastewater. J. Memb. Sci. 501, 45–52.

Shoener, B.D., Zhong, C., Greiner, A.D., Khunjar, W.O., Hong, P.Y., Guest, J.S., 2016. Design of anaerobic membrane bioreactors for the valorization of dilute organic carbon waste streams. Energy Environ. Sci. 9, 1102–1112.

Song, X., Luo, W., Hai, F.I., Price, W.E., Guo, W., Ngo, H.H., Nghiem, L.D., 2018. Resource recovery from wastewater by anaerobic membrane bioreactors: opportunities and challenges. Bioresour. Technol. 270, 669–677.

Stazi, V., Tomei, M.C., 2018. Enhancing anaerobic treatment of domestic wastewater: state of the art, innovative technologies and future perspectives. Sci. Total Environ. 635, 78–91.

Verrecht, B., Maere, T., Nopens, I., Brepols, C., Judd, S., 2010. The cost of a large-scale hollow fibre MBR. Water Res. 44, 5274–5283.
Vinardell, S., Astals, S., Peces, M., Cardete, M.A., Fernández, I., Mata-Alvarez, J., Dosta, J., 2020. Advances in anaerobic membrane bioreactor technology for municipal wastewater treatment: a 2020 updated review. Renew. Sust. Energ. Rev. 130, 109936.
Vinardell, S., Dosta, J., Mata-Alvarez, J., Astals, S., 2021. Unravelling the economics behind mainstream anaerobic membrane bioreactor application under different plant layouts. Bioresour. Technol. 319, 124170.
Wang, K.M., Cingolani, D., Eusebi, A.L., Soares, A., Jefferson, B., McAdam, E.J., 2018. Identification of gas sparging regimes for granular anaerobic membrane bioreactor to enable energy neutral municipal wastewater treatment. J. Membr. Sci. 555, 125–133.
Wang, K.M., Soares, A., Jefferson, B., Wang, H.Y., Zhang, L.J., Jiang, S.F., McAdam, E.J., 2020. Establishing the mechanisms underpinning solids breakthrough in UASB configured anaerobic membrane bioreactors to mitigate fouling. Water Res. 176, 115754.
Wang, Z., Ma, J., Tang, C.Y., Kimura, K., Wang, Q., Han, X., 2014. Membrane cleaning in membrane bioreactors: a review. J. Membr. Sci. 468, 276–307.
Xin, C., Cheng, Z., You, Z., Bai, H., Wang, J., 2020. Using EEM fluorescence to characterize the membrane integrity of membrane bioreactor (MBR). J. Membr. Sci. 610, 118356.
Yao, Y., Zhou, Z., Stuckey, D.C., Meng, F., 2020. Micro-particles-a neglected but critical cause of different membrane fouling between aerobic and anaerobic membrane bioreactors. ACS Sustain. Chem. Eng. 8, 16680–16690.
Zhen, G., Pan, Y., Lu, X., Li, Y.-Y., Zhang, Z., Niu, C., Kumar, G., Kobayashi, T., Zhao, Y., Xu, K., 2019. Anaerobic membrane bioreactor towards biowaste biorefinery and chemical energy harvest: recent progress, membrane fouling and future perspectives. Renew. Sust. Energ. Rev. 115, 109392.
Zhou, Z., Tao, Y., Zhang, S., Xiao, Y., Meng, F., Stuckey, D.C., 2019. Size-dependent microbial diversity of sub-visible particles in a submerged anaerobic membrane bioreactor (SAnMBR): implications for membrane fouling. Water Res. 159, 20–29.